

## The effects of sheet dimension on the 3D curved parts rolling based on arc-shaped rollers

Xiang Chang<sup>1,2</sup>, Ming Li<sup>2</sup>, Depeng Sun<sup>1</sup>, Chuandong Chen<sup>2</sup>

<sup>1</sup>Jiangsu Vocational Institute of Architectural Technology, School of Intelligent Manufacturing. Xuzhou, Jiangsu, China.

<sup>2</sup>Jilin University, College of Materials Science and Engineering. Changchun, Jilin, China.

e-mail: hichangx@163.com, 610262248@qq.com, sun.dpeng@163.com, 676522789@qq.com

### ABSTRACT

The rolling of 3D curved parts based on arc-shaped rollers is a new and effective method for forming curved parts with double curvature. In this paper, the spherical parts are taken as an example, and the influence of sheet dimension on the rolling of 3D curved parts is studied for the first time. A series of numerical simulations and experiments are carried out with different sheet dimensions under the same maximum rolling reduction ratio. The effect of the length, width, and thickness of the sheet metal on the longitudinal bending deformation and material utilization of the formed spherical parts was investigated. Numerical simulation and experimental results show that the longitudinal bending deformation of the formed spherical part is not affected by the sheet length, and decreases with the increase of the sheet width, and decreases with the increase of the sheet thickness. The material utilization rate of the formed spherical part increases with the increase of the sheet length, decreases with the increase of the sheet width, and decreases with the increase of the sheet thickness.

**Keywords:** Rolling; 3D curved part; Flexible forming; Numerical simulation.

### 1. INTRODUCTION

3D curved parts rolling with arc-shaped rollers is a new type of 3D curved surface flexible forming technology, used to produce double-curvature surface parts. Double-curvature surface parts are widely used in aviation, aerospace, shipbuilding, high-speed trains, construction, and other industries. Conventional forming technology is mainly used to produce large quantities of single-shaped products. Due to the high mold manufacturing cost and long production cycle, these methods are not suitable for processing multi-variety, small-batch 3D curved parts. However, with the increasing market demand for product diversification and individualization, there is an increasing demand for multi-variety, small-batch 3D curved parts. Many industrial fields have an urgent need for fast and low-cost 3D curved parts forming technology. For these reasons, some scholars have developed a variety of flexible forming techniques [1], such as multi-point forming [2, 3], multi-point stretch forming [4, 5], single-point incremental forming [6, 7], shot peening forming [8, 9], flame bending process [10, 11] and so on.

In recent years, some scholars have proposed several new types of rolling processes for three-dimensional curved parts and conducted in-depth research on them. YAMASHITA and YAMAKAWA [12] first proposed the use of roll forming technology to produce 3D curved parts, and designed a flexible forming device composed of a pair of feed rollers, a pair of discharge rollers and multiple pairs of forming straight rollers. YOON and YANG [13] developed an incremental 3D surface part roll forming process, which is realized by a combination of an upper center roller and two pairs of lower support rollers. LI [14] proposed a continuous flexible forming process using a small-diameter bending roller made of steel wire as the forming roller. SHIM *et al.* [15] proposed an array rolling process for forming 3D curved parts. The forming tool consists of three rows of upper rollers and three rows of lower rollers, and each row of rollers contains several independent short rollers. By reasonably controlling the position of each short roller, the sheet metal can be processed into a curved surface part with double curvature. LI *et al.* [16, 17] proposed a flexible rolling technology that uses only two bendable flexible rollers to produce 3D curved parts. This method uses bendable flexible rollers to form unevenly distributed roll gaps to achieve roll forming of 3D curved parts, and it has high flexibility. By adjusting the bending shape of the flexible work rollers, different types of roll gap shapes can be combined to realize the rolling forming of different types and specifications of 3D curved parts [18–20].

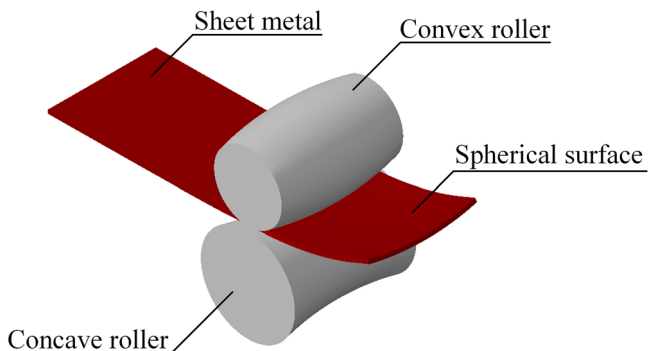


**Figure 1:** 3D curved parts formed by arc-shaped rollers.

Despite many advantages, the flexible rolling forming method using bendable flexible rolls still has some shortcomings: in order to increase the lateral bending effect and realize the torque transmission, the forming device can only use small diameter rollers as forming tools; The diameter of the flexible roll is small, so the torque transmitted is small; and the flexible rollers need to maintain a bent state under the combined action of the force of the sheet metal and the support force of the adjustment mechanism, so the sheet metal must have a certain strength and hardness. The bending state of the forming tool is maintained, and the rolling force provided by the forming tool under the bending stress state is small, so this method is only suitable for cold rolling of sheet metal with low hardness and small thickness. Therefore, WANG *et al.* [21] developed a flexible rolling method by a pair of arc-shaped rollers based on the flexible rolling technology (see Figure 1). In this method, the forming tools are a convex roller and a concave roller. By selecting the appropriate roller, uneven roll gaps of different shapes can be formed, to realize the rolling of 3D curved parts with different specifications and parameters [21].

WANG *et al.* [22] studied the effect of the maximum rolling reduction on the longitudinal bending deformation of formed spherical parts. The results showed that the longitudinal bending deformation of formed spherical parts increased with the increase of the maximum rolling reduction, and proved that the metal sheet can be formed into 3D curved parts with large deformation by using only a small rolling reduction. CHANG *et al.* [23] studied the influence of the minimum rolling reduction on the shape accuracy of formed 3D curved parts. The results show that in order to obtain better shape accuracy of formed parts, the minimum rolling reduction must be ensured to be greater than zero. WANG *et al.* [24] studied the influence of the generatrix radius difference of the rollers on the forming results of spherical parts. The research shows that under the same maximum rolling reduction, the longitudinal bending deformation of spherical parts increases with the increase of the generatrix radius difference of the rollers, and the load required for forming curved parts decreases with the increase of the generatrix radius difference of the rollers. CHANG *et al.* [25] found the cause of instability in the curved parts rolling by analyzing the stress of sheet metal, and proposed the method of using auxiliary plate to improve the stability of the curved parts rolling. CHANG *et al.* [26] proposed a method that can form different types of curved parts through small adjustments of the rolling reduction without replacing the rollers. CHANG *et al.* [27] studied the influence of the central section diameter of the rollers on the forming effect of the formed curved parts. The results showed that the larger the central section diameter of the rollers, the more stable the rolling process and the better the shape accuracy of the formed curved parts; however, excessive roller diameter would inhibit the longitudinal bending deformation of sheet metal. The above research has proved the feasibility of the forming method, and studied the influence of various process parameters on the shape accuracy of the formed 3D curved parts, but did not discuss the influence of sheet size on the forming effect.

In this paper, the concept of dividing the forming area is put forward according to the forming effect of 3D curved parts. The influence of the length, width and thickness of the sheet metal on the forming area is studied in detail. A series of numerical simulations and experiments were carried out with different sheet dimensions under the same maximum rolling reduction ratio. The influence of different sheet dimensions on the stable forming area of the formed spherical part is compared and analyzed. According to the length of the stable forming area of the formed parts along the rolling direction, the influence of the sheet dimension on the material utilization rate of the formed spherical part is analyzed.

## 2. FORMING MECHANISM OF 3D CURVED PARTS ROLLING BASED ON ARC-SHAPED ROLLERS

The smooth and continuous arc-shaped roller ensures the good surface quality of the formed 3D curved parts. When forming spherical parts, the roll gap at the center of the rollers is the smallest and gradually increases from the center to the edges on both sides. The uneven distribution of the roll gap causes the longitudinal extension

of the sheet metal to gradually decrease from the center to the edges on both sides during the rolling process, which causes longitudinal bending deformation. Simultaneously, due to the curved shape of the roll gap in the transverse direction (perpendicular to the rolling direction), the sheet metal produces transverse bending deformation. Therefore, a double-curvature curved part is formed.

Due to the continuity of the metal sheet, in the presence of transverse bending deformation, the uneven extension of the sheet in the longitudinal direction causes the longitudinal bending of the sheet to form a 3D curved surface part. The transverse shape of the three-dimensional curved part mainly depends on the curved profile of the forming rollers, and the transverse curvature  $\rho_T$  mainly depends on the arc radius of the upper and lower work rollers. The longitudinal bending deformation is caused by the uneven extension of the metal sheet in the longitudinal direction during the forming process. When ignoring the stretch in the width direction of the sheet metal, the longitudinal curvature  $\rho_L$  is determined by the relative elongation of the sheet in the longitudinal direction.

Due to the uneven roll gap, the longitudinal elongation of the sheet at different positions on the same cross section is different. If the length at point  $z$  is recorded as  $l(z)$ , then the longitudinal strain increment at that point can be expressed as:

$$d\varepsilon_L(z) = d(\Delta l) / \Delta l \quad (1)$$

Since the main direction of strain remains unchanged during the deformation process, the total strain can be obtained:

$$\varepsilon_L(z) = \int_{\Delta l_0}^{\Delta l} \frac{d(\Delta l)}{\Delta l} = \ln \frac{\Delta l(z)}{\Delta l_0} \quad (2)$$

Therefore, the length of the sheet metal with length  $\Delta l_0$  after rolling deformation can be expressed as:

$$\Delta l(z) = \Delta l_0 \exp[\varepsilon_L(z)] \quad (3)$$

After the sheet with a length of  $\Delta l_0$  is rolled and deformed, the longitudinal curvature at any point  $z$  on its surface can be expressed by its longitudinal extension as:

$$\rho_L = \frac{d\theta}{dl} \quad (4)$$

In Equation 4,  $\theta$  is the inclination angle of the longitudinal curve along the normal line of the sheet material after deformation. Therefore, the length of the sheet with length  $\Delta l_0$  after rolling deformation can also be expressed as:

$$\Delta l(z) = \int_0^{\Delta\theta} \frac{d\theta}{\rho_L} \approx \frac{\Delta\theta(z)}{\rho_L(z)} \quad (5)$$

In Equation 5,  $\rho_L(z)$  is the average longitudinal curvature of the sheet after deformation,  $\Delta\theta(z)$  is the normal dip angle of the surface after deformation of the sheet. From Equations 3 and 5, we can get:

$$\rho_L = \frac{\Delta\theta(z)}{\Delta l_0 \exp[\varepsilon_L(z)]} \quad (6)$$

Integrating the longitudinal curvature  $\rho_L$  can obtain the curve of the rolled surface along the longitudinal direction.

### 3. FINITE ELEMENT MODEL

In order to further study the rolling process of the 3D curved parts based on arc-shaped rollers, an elastic-plastic finite element (FE) model was established by the FE numerical simulation software Abaqus/Explicit. The FE

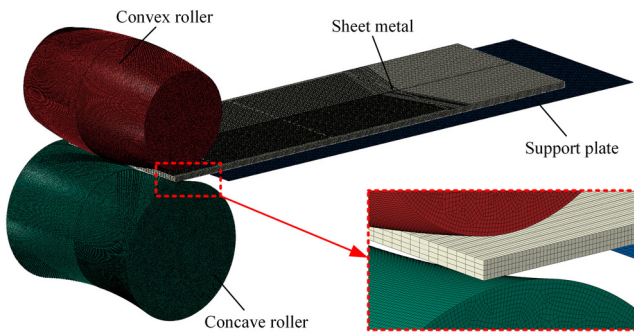


**Figure 2:** Finite element model of the rolling of 3D curved parts with arc-shaped rollers.

**Table 1:** Material properties of 1060-O aluminum in FEM at room temperature.

MATERIAL	DENSITY (kg/m <sup>3</sup> )	ELASTIC MODULUS (MPa)	POISSON'S RATIO	YIELD LIMIT (MPa)
A1060-O	2705	69000	0.33	28

model is composed of a sheet metal, a convex roller, a concave roller and a support plate (see Figure 2). The sheet metal is modeled as a deformable body, and the C3D8R solid element (eight-node linear brick, reduced integration, hourglass control) is used to mesh it. The sheet metal is divided into 4 layers in the thickness direction, and its mesh sizes in the length and width directions are 0.6 mm and 1.8 mm, respectively. The material of the sheet metal is set with the properties of 1060-O aluminum alloy, and its properties at room temperature are shown in Table 1. The generatrix radii of the convex roller and the concave roller are 206 and 212 mm, respectively. Because the deformation of the rollers and the support plate can be ignored, they are modeled as discrete rigid bodies. In order to improve the accuracy of calculation, the mesh size of discrete rigid bodies is set to  $0.6 \times 0.6$  mm. The angle velocity of the rollers is set to 10rad/s, which is selected according to the quasi-static conditions of the sheet metal forming process in the Abaqus software. The rolling reduction is controlled by controlling the downward distance of the convex roller, and the maximum compression ratio in all the finite element models in this paper is controlled to 2% of the sheet thickness. Using the penalty friction formula and the Coulomb friction model, according to engineering experience, the friction coefficient is assumed to be 0.12. Due to the symmetrical structure of the sheet metal and rollers, and symmetrical boundary and load conditions, a 1/2 model is used for calculation to improve efficiency.

#### 4. ANALYSIS OF NUMERICAL SIMULATION RESULTS

##### 4.1. Division of the forming area

In order to analyze the influence of the size of the sheet metal on the utilization ratio of the formed spherical part, the formed spherical part was divided into three regions along the longitudinal direction according to the distribution law of the strain in the thickness direction. Figure 3 shows the thickness-direction strain distribution of a convex curved part formed by rigid arc-shaped rollers. The thickness-direction strain of the formed spherical part gradually decreases from the center to the edges in transverse direction (perpendicular to the rolling direction); the thickness strain in the longitudinal direction (rolling direction) changes significantly near the front and rear ends, and remains stable in the middle region away from the both ends (see Figure 3).

Figure 4 shows the transverse curvature radius and longitudinal curvature radius of the formed spherical part along the longitudinal direction. The longitudinal curvature radius gradually decreases in the front transition area, remains stable in the stable forming area, and gradually increases in the rear transition area. The transverse curvature radius slowly decreases in the front transition area, remains stable in the stable forming area, and slowly decreases in the rear transition area. Because the stable forming area of the transverse curvature radius and the longitudinal curvature radius of the formed spherical part coincide, and the change of the transverse radius of curvature is small. Therefore, this paper divides different forming areas by the change trend of the longitudinal curvature radius, and calculates the material utilization ratio with different sheet size. And when the influence of the sheet metal size on the longitudinal curvature radius of the formed spherical part is analyzed

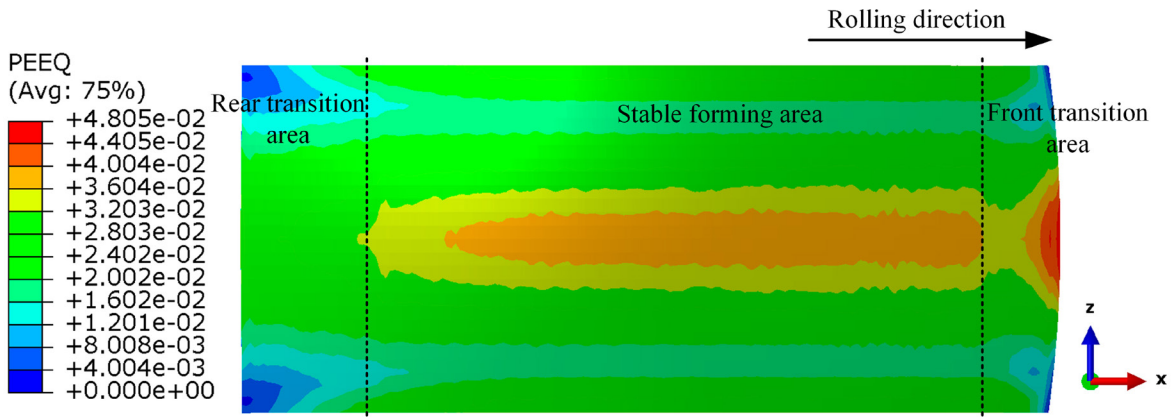


**Figure 3:** Division of the forming area.

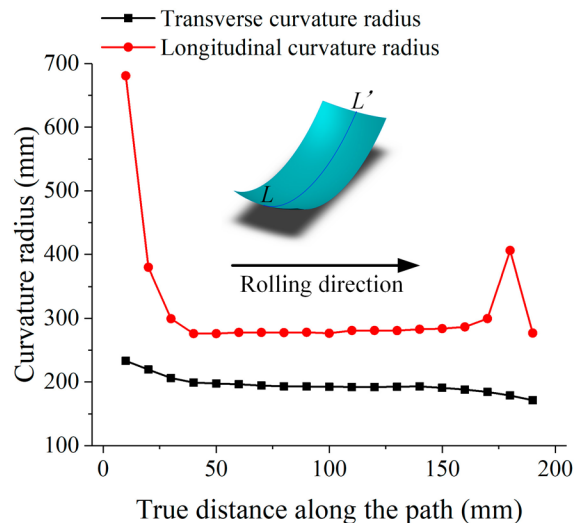


**Figure 4:** Transverse and longitudinal curvature radius of the formed spherical part.

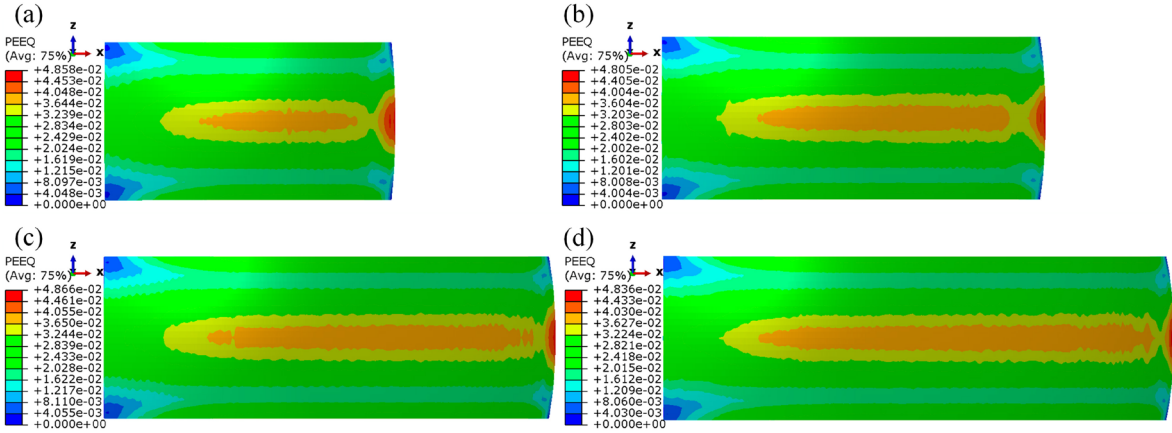
below, the longitudinal curvature radius is the longitudinal curvature radius of the stable forming area of the formed spherical part.

#### 4.2. Effect of the sheet length

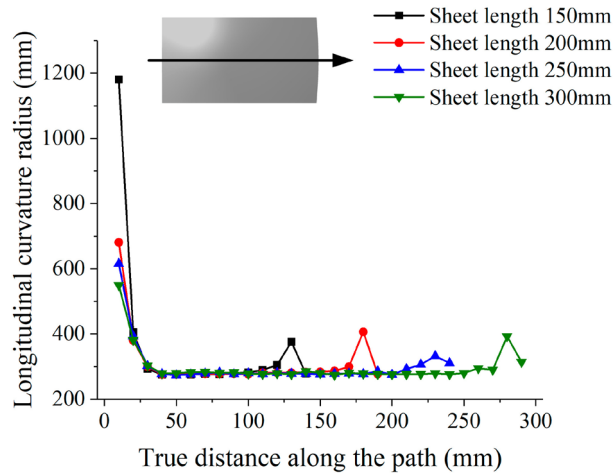
A series of finite element models were established, with dimensions (length  $\times$  width  $\times$  thickness) of  $150 \times 80 \times 2.5$ ,  $200 \times 80 \times 2.5$ ,  $250 \times 80 \times 2.5$  and  $300 \times 80 \times 2.5$  mm, to investigate the effect of sheet length on longitudinal bending deformation and the material utilization ratio of formed spherical parts. The equivalent plastic strain of the formed spherical parts is shown in Figure 5. The equivalent plastic strain in the stable forming area of the formed part is continuously distributed in strips along the longitudinal direction, indicating that the forming effect is good. The equivalent plastic strain of the stable forming area of each formed part is basically the same, and the length of the stable forming area increases with the increase of the sheet length.

Figure 6 shows the distribution of the longitudinal curvature radius of each forming part along the forming direction. It can be found that the longitudinal curvature radius of the stable forming area for the formed parts with different lengths is the same, indicating that the longitudinal bending deformation of the formed curved part is not affected by the sheet length.

The length of the different forming areas for the formed parts and their material utilization ratio are shown in Figure 7. The length of front and rear transition area of the formed parts is not affected by the sheet length, and the length of stable forming area increases with the increase of the sheet length. Therefore, the material utilization ratio of the formed parts increases with the increase of the sheet length.



**Figure 5:** Equivalent plastic strain with different sheet lengths: (a) 150 mm, (b) 200 mm, (c) 250 mm and (d) 300 mm.



**Figure 6:** Longitudinal curvature radius with different sheet lengths.

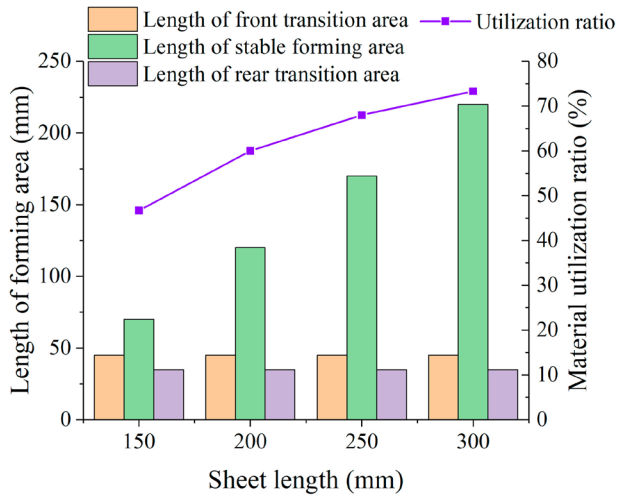


**Figure 7:** Length of forming area and material utilization ratio with different sheet lengths.

#### 4.3. Effect of the sheet width

A series of finite element models were established, with dimensions (length  $\times$  width  $\times$  thickness) of  $250 \times 60 \times 2.5$ ,  $250 \times 80 \times 2.5$ ,  $250 \times 100 \times 2.5$  and  $250 \times 120 \times 2.5$  mm, to investigate the effect of sheet width on longitudinal bending deformation and the material utilization ratio of formed spherical parts. The equivalent plastic

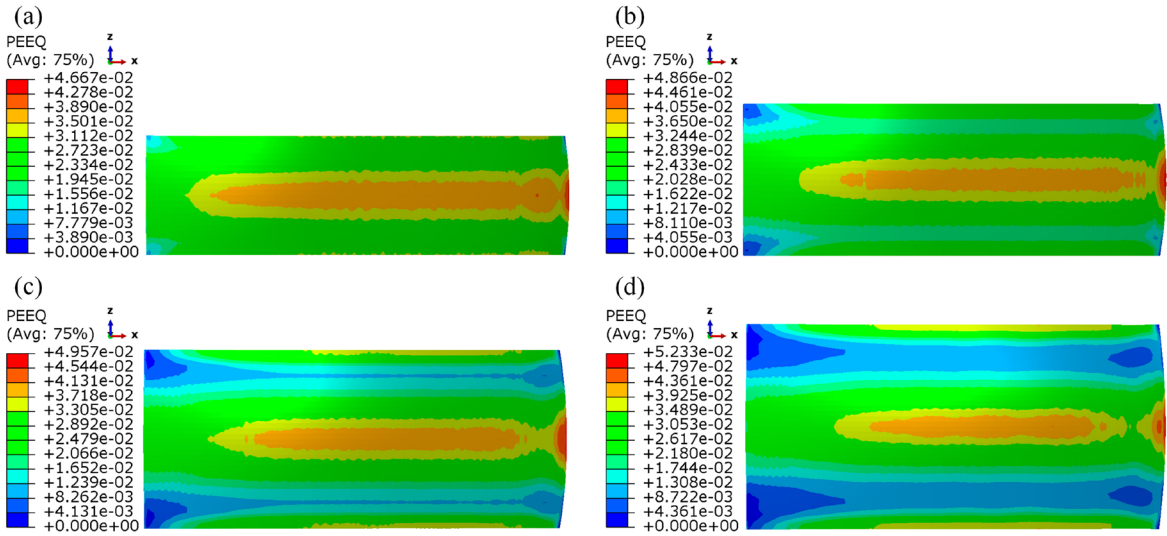


**Figure 8:** Equivalent plastic strain with different sheet widths: (a) 60 mm, (b) 80 mm, (c) 100 mm and (d) 120 mm.

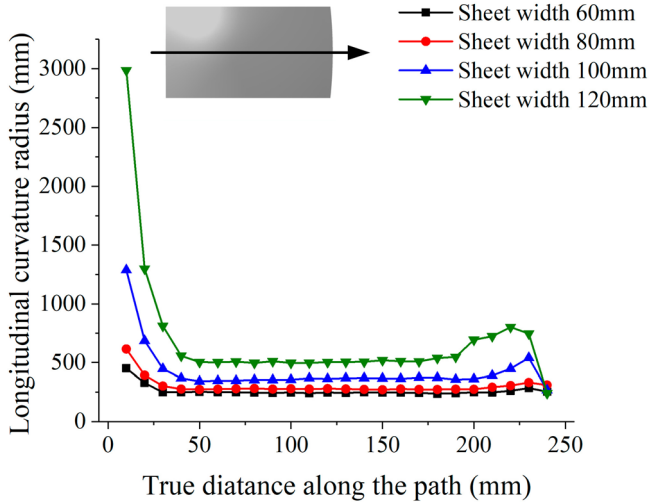


**Figure 9:** Distribution of longitudinal curvature radius of different sheet widths.

strain at the center of each formed part increases slightly with the increase of the sheet width, but the equivalent plastic strain at the edge of the wider metal plate is smaller (see Figure 8). The smaller plastic strain at the edge of the sheet will limit its longitudinal bending deformation.

Figure 9 shows the distribution of the longitudinal curvature radius of each formed spherical part along their forming direction. It can be found that the longitudinal curvature radius of the formed parts increases with the increase of the sheet width, indicating that the forming difficulty increases with the increase of the sheet width under the same process parameters.

The length of the different forming areas for the formed parts with different sheet widths and their material utilization ratio are shown in Figure 10. The front and rear transition areas both increase with the increase of the sheet width, resulting in the length of stable forming area decreases with the increase of the sheet width. Therefore, the material utilization ratio decreases as the sheet width increases. The larger sheet width, the larger contact area between the rollers and the sheet metal, resulting in a smaller compression ratio at the edge of the sheet. Under the condition that the center rolling reduction is constant, the increase of the sheet width makes the difference between the center and the edge compression ratio of the sheet larger, and the additional stress on the edge of the sheet is not enough to bend itself to the target shape. Therefore, the length of the transition areas increases with the increase of the sheet width, and the percentage of the stable forming area in the sheet length decreases with the increase of the sheet width, and the material utilization ratio decreases.

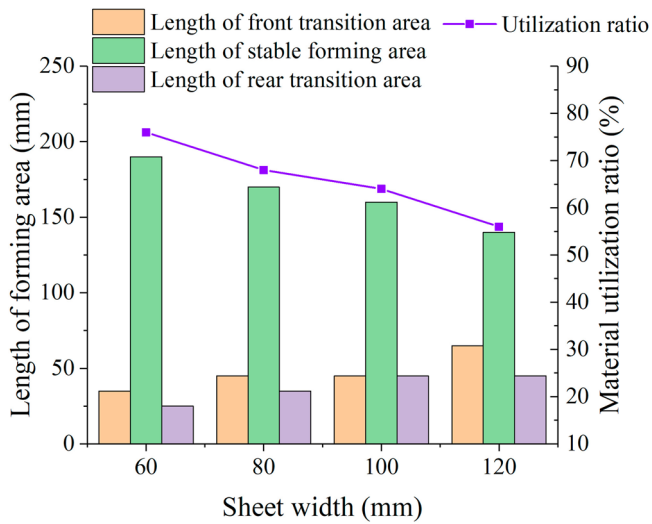


**Figure 10:** Length of forming area and material utilization ratio with different sheet widths.

#### 4.4. Effect of sheet thickness

Established finite element models with sheet size (length  $\times$  width  $\times$  thickness) of  $250 \times 80 \times 1.5$ ,  $250 \times 80 \times 2.0$ ,  $250 \times 80 \times 2.5$  and  $250 \times 80 \times 3.0$  mm to investigate the effect of sheet thickness on the longitudinal bend deformation and the material utilization ratio of formed spherical parts. The equivalent plastic strain of formed spherical parts with different sheet thicknesses is shown in Figure 11, which indicates that the length of stable forming area decreases with the increase of sheet thickness.

From the distribution of the longitudinal curvature radius of the formed parts (see Figure 12), it can be seen that under the same maximum rolling compression rate, the longitudinal bending deformation of the formed spherical part and the length of the stable forming area decrease with the increase of the sheet thickness. The length of the different forming areas for the formed parts with different sheet thicknesses and their material utilization ratio are shown in Figure 13. The front and rear transition areas both increase with the increase of the sheet thickness, resulting in the length of the stable forming area decreases with the increase of the sheet thickness. Therefore, the material utilization ratio decreases as the sheet thickness increases. In the case of the same maximum rolling compression rate, the thicker the sheet, the greater the additional stress required to bend itself into the target shape. Therefore, as the sheet thickness increases, the additional stress in the transition area at both ends is not enough to bend it into the target shape, resulting in the length of the transition area increasing with the increase of the sheet thickness, and the length of the stable forming area decrease with the increase of the sheet thickness. As a result, the material utilization ratio decreases as the sheet thickness increases.

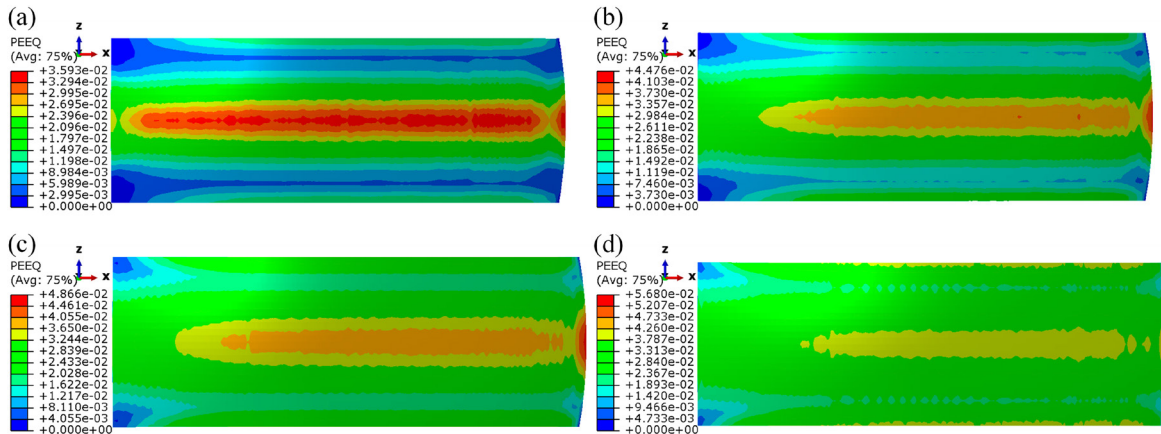


**Figure 11:** Equivalent plastic strain with different sheet thicknesses: (a) 1.5 mm, (b) 2.0 mm, (c) 2.5 mm and (d) 3.0 mm.

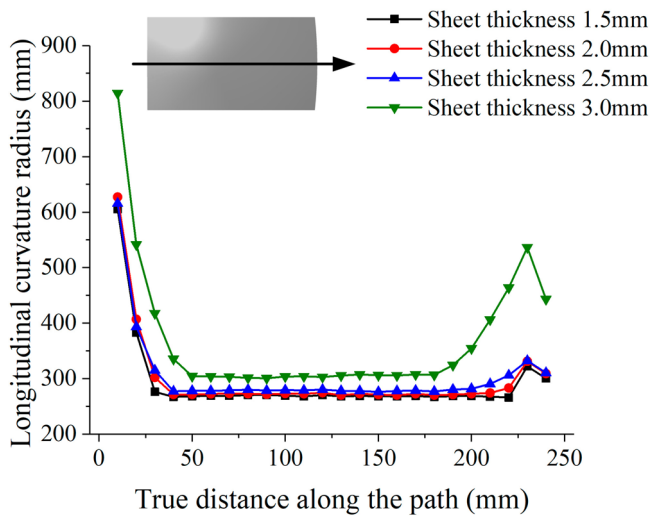


**Figure 12:** Distribution of longitudinal curvature radius of different sheet thicknesses.

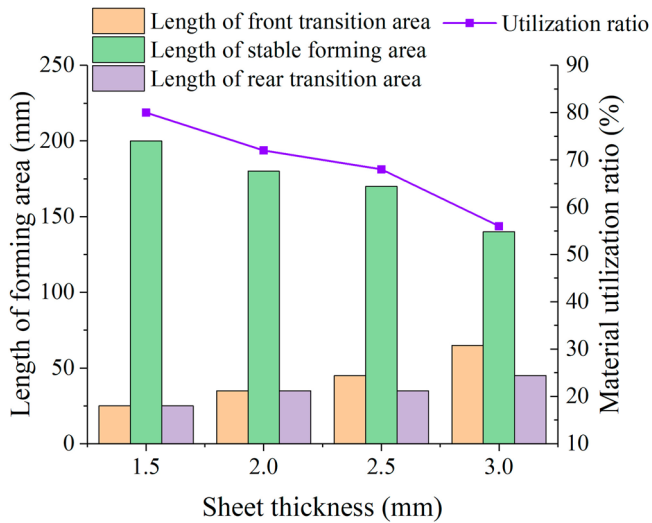


**Figure 13:** Length of forming area and material utilization ratio with different sheet thicknesses.

## 5. EXPERIMENTAL INVESTIGATIONS

### 5.1. Experimental and testing equipment

The rolling equipment of 3D curved parts is shown in Figure 14a. The forming tool of the equipment is a pair of rigid arc-shaped rollers. The upper roller is a convex roller and the lower roller is a concave roller, and the rollers can be quickly disassembled and replaced. The device can precisely adjust the vertical motion of the convex roller through the worm gear mechanism. When the control shaft rotates once, the convex roller moves 0.01 mm. Before rolling, the convex roller is adjusted to a predetermined position according to the initial size of the sheet metal and the curvature radius of the target 3D parts. Then, through the motor and synchronous transmission mechanism, the rollers are driven to rotate synchronously, so that the sheet metal is bitten into the roll gap by friction. The material of the metal plate used in the experiment is 1060 aluminum in annealed state. The formed spherical parts were measured by the NDI Procam 3000 3D laser scanner (see Figure 14b). And the reliability of the finite element numerical simulation results can be confirmed through the experimental results.

### 5.2. Experimental research on the effect of sheet length

Sheet metals with dimensions (length × width × thickness) of 200 × 80 × 2, 250 × 80 × 2 and 300 × 80 × 2 mm were used to conduct experiments to investigate the influence of sheet length on the formed spherical parts. The

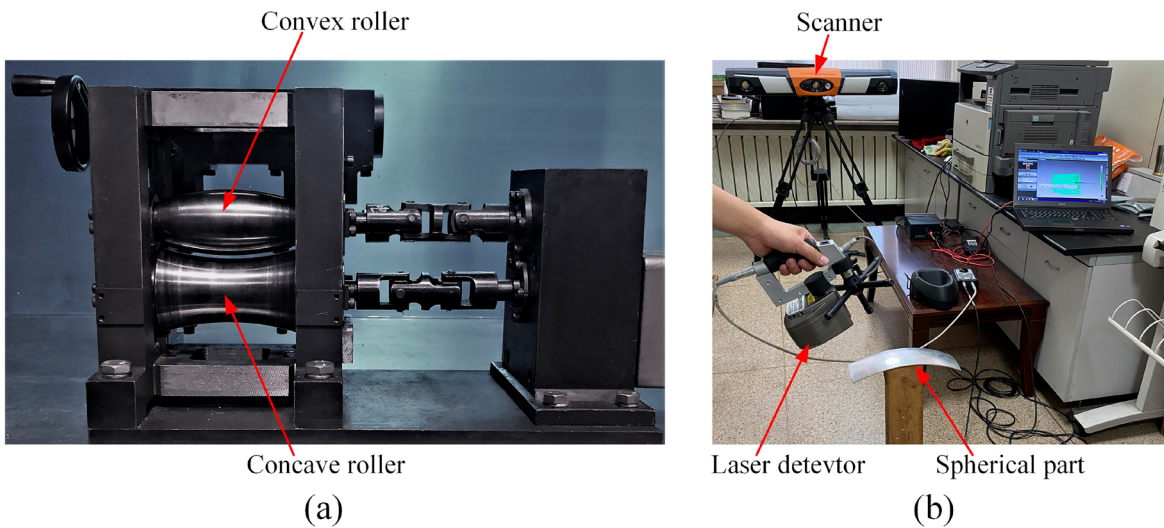


**Figure 14:** Experimental and testing equipment: (a) Rolling equipment of 3D curved parts; (b) NDI Procam 3000 3D laser scanner.

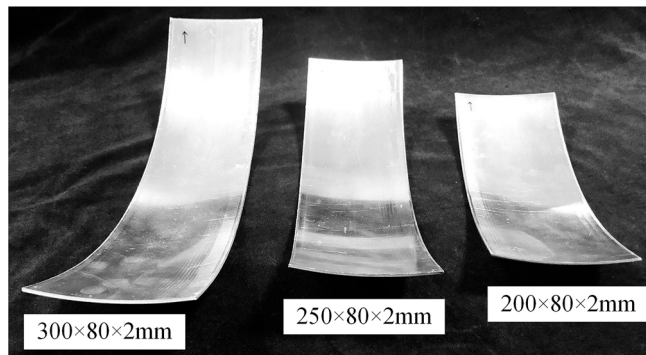


**Figure 15:** Experimental processed parts with different sheet lengths.

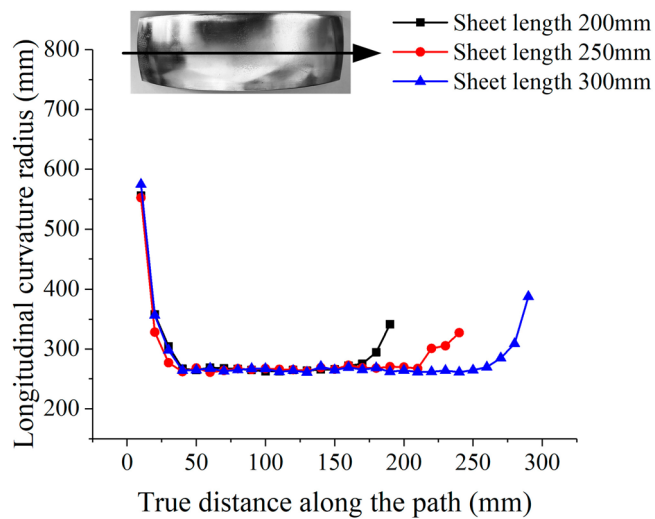


**Figure 16:** Longitudinal curvature radius of experimental processed parts with different sheet lengths.

surfaces of the processed spherical parts are all smooth without wrinkles, and the forming effect is good (see Figure 15). The distribution of the longitudinal curvature radius of the workpiece along the forming direction is shown in Figure 16. The longitudinal curvature radius of the stable forming area is equal, indicating that the effective longitudinal bending deformation is not affected by the sheet length. The length of each forming area and the material utilization ratio are shown in Figure 17. The length of the front and rear transition area is not

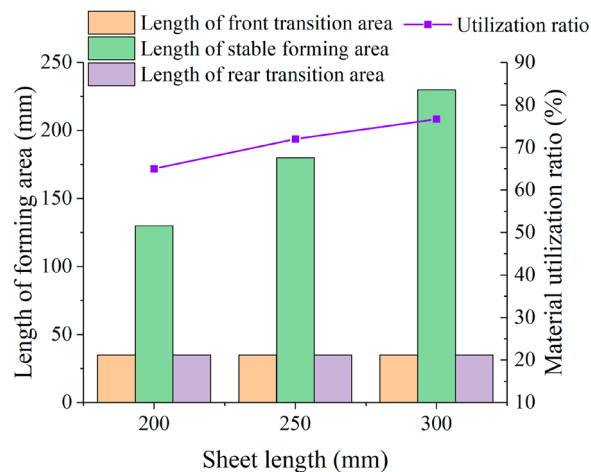


**Figure 17:** Utilization ratio of experimental processed parts with different sheet lengths.

affected by the sheet length, resulting in the increase of the length of the stable forming area with the increase of the sheet length, so the material utilization rate increases with the increase of the sheet length. The experimental results are consistent with the finite element numerical simulation results.

### 5.3. Experimental research on the effect of sheet width

Sheet metals with dimensions (length  $\times$  width  $\times$  thickness) of  $300 \times 80 \times 2$ ,  $300 \times 100 \times 2$  and  $300 \times 120 \times 2$  mm were used to conduct experiments to investigate the influence of sheet width on the formed spherical parts (see Figure 18). After measurement, the longitudinal curvature radius distribution of the processed parts is shown in Figure 19. The wider the sheet metal, the smaller the longitudinal bending deformation of the formed spherical

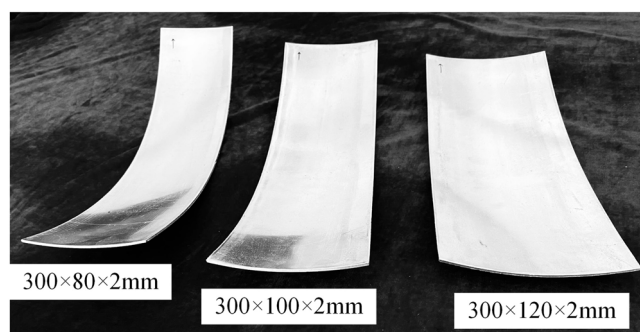


**Figure 18:** Experimental processed parts with different sheet widths.

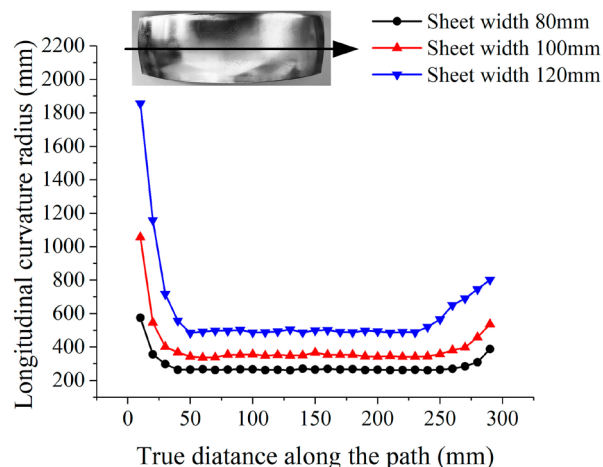


**Figure 19:** Longitudinal curvature radius of experimental processed parts with different sheet widths.

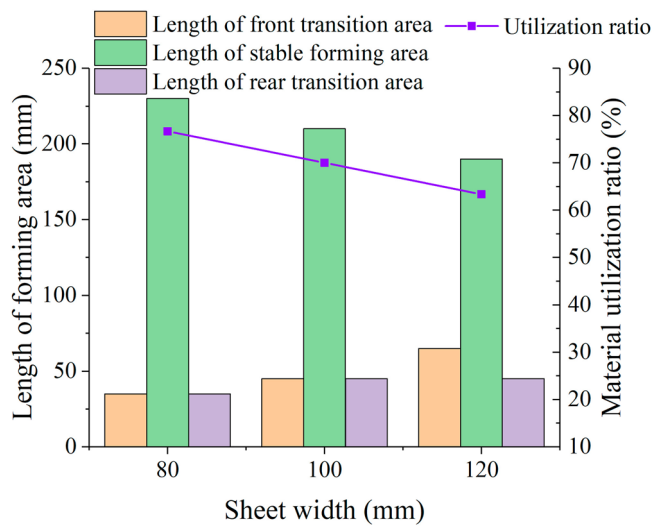


**Figure 20:** Utilization ratio of experimental processed parts with different sheet widths.

part. The length of the transition areas increases with the increase of the sheet width, and the length of the stable forming area decreases with the increase of the sheet width, resulting in the material utilization ratio decreases as the increases of the sheet width (see Figure 20). The experimental results of the sheet width are consistent with the numerical simulation results.

#### 5.4. Experimental research on the effect of sheet width

Sheet metals with dimensions (length  $\times$  width  $\times$  thickness) of  $300 \times 80 \times 1.5$ ,  $300 \times 80 \times 2$  and  $300 \times 80 \times 2.5$  mm were used to conduct experiments to investigate the influence of sheet thickness on the formed spherical parts

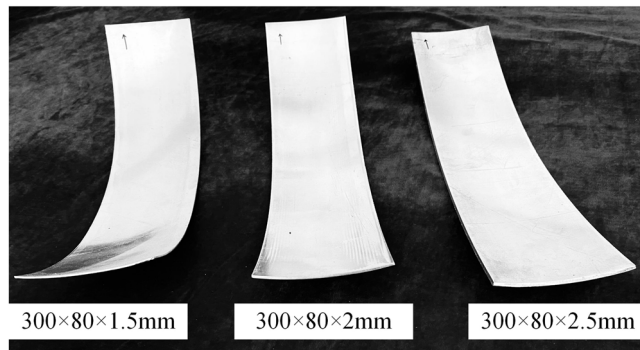


**Figure 21:** Experimental processed parts with different sheet thicknesses.

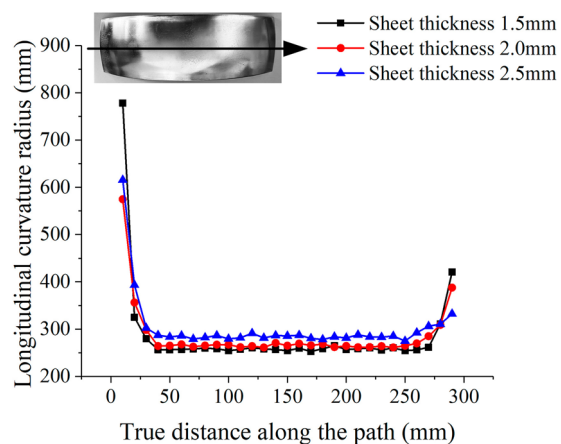


**Figure 22:** Longitudinal curvature radius of experimental processed parts with different sheet thicknesses.

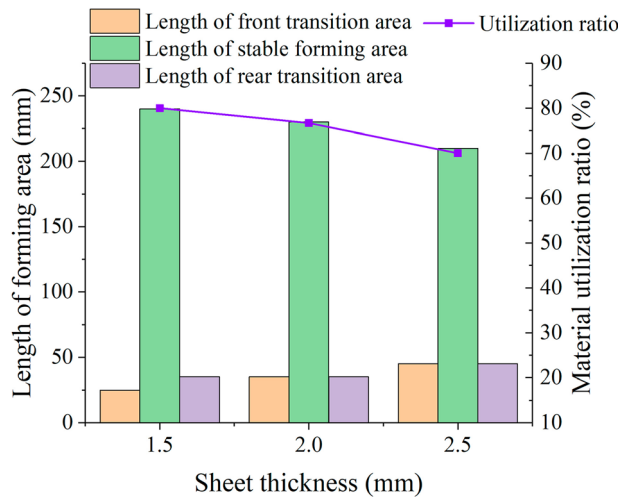


**Figure 23:** Utilization ratio of experimental processed parts with different sheet thicknesses.

(see Figure 21). The longitudinal curvature radius of each formed part is shown in Figure 22. The longitudinal curvature radius of the stable forming area increases with the increase of the sheet thickness, indicating that the larger the sheet thickness, the smaller the longitudinal bending deformation of the formed curved part under the same rolling compression rate. The length of each forming area and material utilization of the formed parts are shown in Figure 23. The length of the front and the rear transition area increases with the increase of the sheet thickness, and the length of the stable forming area decreases with the increase of the sheet thickness. The material utilization ratio decreases as the sheet thickness increases. The experimental results about the influence of sheet thickness on the formed spherical parts are consistent with the numerical simulation results.

## 6. CONCLUSIONS

In this paper, taking the rolling of spherical parts as an example, the influence of sheet dimensions on the longitudinal bending deformation and material utilization ratio of the 3D curved parts formed by arc-shaped rollers is studied for the first time. A series of numerical simulations and experiments were carried out to investigate the effects of sheet length, sheet width and sheet thickness on the longitudinal bending deformation and material utilization ratio of the formed spherical part. The research results are summarized as follows:

1. The longitudinal bending deformation in the stable forming area of the formed spherical part is not affected by the sheet length. However, the length of the stable forming area increases with the increase of the sheet length, namely the material utilization rate increases with the increase of the plate length;
2. The longitudinal bending deformation of the stable forming area of the formed spherical part decreases with the increase of the sheet width. The length of the stable forming area decreases with the increase of the sheet width, resulting in the material utilization rate decreases with the increase of the sheet width;
3. The longitudinal bending deformation of the stable forming area of the formed spherical part decreases with the increase of the sheet thickness. The length of the stable forming area decreases with the increase of the sheet thickness, resulting in the material utilization rate decreases with the increase of the sheet thickness.

## 7. ACKNOWLEDGMENTS

The authors appreciate the generous support from Jilin University. The authors appreciate all the anonymous referees for their valuable suggestions, which have helped us to improve the quality of the present manuscript.

## 8. BIBLIOGRAPHY

- [1] ALLWOOD, J.M., UTSUNOMIYA, H., "A survey of flexible forming processes in Japan", *International Journal of Machine Tools & Manufacture*, v. 46, n. 15, pp. 1939–1960, 2006. doi: <http://doi.org/10.1016/j.ijmachtools.2006.01.034>.
- [2] LI, M.Z., CAI, Z.Y., SUI, Z., et al., "Multi-point forming technology for sheet metal", *Journal of Materials Processing Technology*, v. 129, n. 1–3, pp. 333–338, 2002. doi: [http://doi.org/10.1016/S0924-0136\(02\)00685-4](http://doi.org/10.1016/S0924-0136(02)00685-4).

- [3] LI, M.Z., LIU, Y.H., SU, S.Z., et al., "Multi-point forming: a flexible manufacturing method for a 3-d surface sheet", *Journal of Materials Processing Technology*, v. 87, n. 1–3, pp. 277–280, 1999. doi: [http://doi.org/10.1016/S0924-0136\(98\)00364-1](http://doi.org/10.1016/S0924-0136(98)00364-1).
- [4] WALCZYK, D.F., LAKSHMIKANTHAN, J., KIRK, D.R., "Development of a reconfigurable tool for forming aircraft body panels", *Journal of Manufacturing Systems*, v. 17, n. 4, pp. 287–296, 1998. doi: [http://doi.org/10.1016/S0278-6125\(98\)80076-9](http://doi.org/10.1016/S0278-6125(98)80076-9).
- [5] CAI, Z.Y., WANG, S.H., XU, X.D., et al., "Numerical simulation for the multi-point stretch forming process of sheet metal", *Journal of Materials Processing Technology*, v. 209, n. 1, pp. 396–407, 2009. doi: <http://doi.org/10.1016/j.jmatprotec.2008.02.010>.
- [6] DURANTE, M., FORMISANO, A., LAMBIASE, F., "Formability of polycarbonate sheets in single-point incremental forming", *International Journal of Advanced Manufacturing Technology*, v. 102, n. 5–8, pp. 2049–2062, 2019. doi: <http://doi.org/10.1007/s00170-019-03298-w>.
- [7] WU, S., MA, Y.W., GAO, L.T., et al., "A novel multi-step strategy of single point incremental forming for high wall angle shape", *Journal of Manufacturing Processes*, v. 56, pp. 697–706, 2020. doi: <http://doi.org/10.1016/j.jmapro.2020.05.009>.
- [8] WANG, T., PLATTS, M.J., LEVERS, A., "A process model for shot peen forming", *Journal of Materials Processing Technology*, v. 172, n. 2, pp. 159–162, 2006. doi: <http://doi.org/10.1016/j.jmatprotec.2005.09.006>.
- [9] RUSSIG, C., BAMBACH, M., HIRT, G., et al., "Shot peen forming of fiber metal laminates on the example of GLARE®", *International Journal of Material Forming*, v. 7, n. 4, pp. 425–438, 2014. doi: <http://doi.org/10.1007/s12289-013-1137-8>.
- [10] HEMMATI, S.J., SHIN, J.G., "Estimation of flame parameters for flame bending process", *International Journal of Machine Tools & Manufacture*, v. 47, n. 5, pp. 799–804, 2007. doi: <http://doi.org/10.1016/j.ijmachtools.2006.09.005>.
- [11] SAFARI, M., FARZIN, M., "A comparative study on two different irradiating schemes for flame forming of a bowl-shaped surface", *International Journal of Advanced Manufacturing Technology*, v. 80, n. 1–4, pp. 199–207, 2015. doi: <http://doi.org/10.1007/s00170-015-6977-6>.
- [12] YAMASHITA, I., YAMAKAWA, T., U.S. Patent 4770017 apparatus for forming plate with a double-curved surface, Washington, D.C., 13 Sept. 1988.
- [13] YOON, S.J., YANG, D.Y., "Development of a highly flexible incremental roll forming process for the manufacture of a doubly curved sheet metal", *CIRP Annals*, v. 52, n. 1, pp. 201–204, 2003. doi: [http://doi.org/10.1016/S0007-8506\(07\)60565-4](http://doi.org/10.1016/S0007-8506(07)60565-4).
- [14] LI, M., "Method of multipoint continuous forming for the freeform surface parts", *Jixie Gongcheng Xuebao*, v. 43, n. 12, pp. 155–159, 2007. doi: <http://doi.org/10.3901/JME.2007.12.155>.
- [15] SHIM, D.S., YANG, D.Y., KIM, K.H., et al., "Numerical and experimental investigation into cold incremental rolling of doubly curved plates for process design of a new LARS (line array roll set) rolling process", *CIRP Annals*, v. 58, n. 1, pp. 239–242, 2009. doi: <http://doi.org/10.1016/j.cirp.2009.03.112>.
- [16] LI, M.Z., CAI, Z.Y., LI, R.J., et al., "Continuous forming method for three-dimensional surface parts based on the rolling process using bended roll", *Journal of Mechanical Engineering*, v. 48, pp. 44–49, 2012. doi: <http://doi.org/10.3901/JME.2012.18.044>.
- [17] LI, R.J., LI, M.Z., QIU, N.J., et al., "Surface flexible rolling for three-dimensional sheet metal parts", *Journal of Materials Processing Technology*, v. 214, n. 2, pp. 380–389, 2014. doi: <http://doi.org/10.1016/j.jmatprotec.2013.09.008>.
- [18] WANG, D.M., LI, M.Z., CAI, Z.Y., "Research on forming precision of flexible rolling method for three-dimensional surface parts through simulation", *International Journal of Advanced Manufacturing Technology*, v. 71, n. 9–12, pp. 1717–1727, 2014. doi: <http://doi.org/10.1007/s00170-013-5581-x>.
- [19] GHIABAKLOO, H., KIM, J., KANG, B.S., "Specialized finite elements for numerical simulation of the flexibly-reconfigurable roll forming process", *International Journal of Mechanical Sciences*, v. 151, pp. 133–153, 2019. doi: <http://doi.org/10.1016/j.ijmecsci.2018.11.002>.
- [20] GHIABAKLOO, H., PARK, J.W., KIL, M.G., et al., "Design of the flexibly-reconfigurable roll forming process by a progressively-improving goal seeking approach", *International Journal of Mechanical Sciences*, v. 157–158, pp. 136–149, 2019. doi: <http://doi.org/10.1016/j.ijmecsci.2019.04.020>.

- [21] WANG, X.T., LI, M.Z., “Research on three-dimensional curved surface rolling based on rigid arc-shaped rollers”, *International Journal of Advanced Manufacturing Technology*, v. 107, n. 1–2, pp. 805–814, 2020. doi: <http://doi.org/10.1007/s00170-020-05096-1>.
- [22] WANG, X.T., LI, M.Z., CHANG, X., “Influence of thickness reduction on the forming results in the three-dimensional surface rolling process with rigid arc-shaped rollers”, *International Journal of Advanced Manufacturing Technology*, v. 114, n. 7–8, pp. 2397–2405, 2021. doi: <http://doi.org/10.1007/s00170-021-07024-3>.
- [23] CHANG, X., FU, W.Z., LI, M.Z., et al., “An investigation into the effect of rolling reduction on 3D curved parts rolling process”, *Metals*, v. 11, n. 8, pp. 1209–1211, 2021. doi: <http://doi.org/10.3390/met11081209>.
- [24] WANG, X., LI, M., LIU, Y., et al., “Influence of the axial radius of rigid arc-shaped rollers in 3D surface rolling”, *Journal of Mechanical Science and Technology*, v. 35, n. 8, pp. 3579–3589, 2021. doi: <http://doi.org/10.1007/s12206-021-0729-3>.
- [25] CHANG, X., FU, W.Z., LI, M.Z., et al., “The flexible rolling process of three-dimensional curved parts using an auxiliary plate based on rigid arc-shaped rollers”, *International Journal of Advanced Manufacturing Technology*, v. 116, n. 3–4, pp. 1103–1113, 2021. doi: <http://doi.org/10.1007/s00170-021-07512-6>.
- [26] CHANG, X., FU, W.Z., LI, M.Z., et al., “Research on rolling different types of 3D curved parts by small adjustments in rolling reduction”, *International Journal of Advanced Manufacturing Technology*, v. 119, n. 9–10, pp. 6235–6244, 2022. doi: <http://doi.org/10.1007/s00170-021-08519-9>.
- [27] CHANG, X., FU, W.Z., LI, M.Z., et al., “The effects of central cross-section diameters of rollers on doubly curved surface rolling”, *International Journal of Advanced Manufacturing Technology*, v. 126, n. 7–8, pp. 3083–3092, 2023. doi: <http://doi.org/10.1007/s00170-023-11295-3>.